

Solutions of the Wick-Cutkosky model in the Light Front Dynamics

Mariane Mangin-Brinet, Jaume Carbonell

Institut des Sciences Nucléaires 53, Av. des Martyrs, 38026 Grenoble, France

Abstract

We study relativistic effects in a system of two scalar particles interacting via a scalar exchange in the Light Front Dynamics framework. The results are compared to those provided by Bethe-Salpeter and non relativistic equations. It is found in particular that for massive exchange, the relativistic description is of crucial importance even in the limit of zero binding energy.

PACS: 11.10, 03.70, 03.65P

Keywords: Light-Front Dynamics, Relativistic equations, Quantum Field Theory

1 Introduction

Light Front Dynamics (LFD) is a field theoretically inspired hamiltonian approach specially well adapted for describing relativistic composite systems. First suggested by Dirac [1] it has been since widely developed (see [2–6] and references therein) and recently applied with success in its explicitly covariant version [7] to the high momentum processes measured in TJNAF [5,8]. In this approach the state vector is defined on a space-time hyperplane given by $\omega \cdot x = \sigma$ where $\omega = (1, \hat{n})$ is a light-like four-vector.

We present here the first results obtained within this approach for the Wick-Cutkosky model [9]. This model describes the dynamics of two identical scalar particles of mass m interacting by the exchange of a massless scalar particle. This first step towards more realistic systems constitutes an instructive case and is presently considered by several authors [10–14]. The model has been extended to the case where the exchanged particle has non zero mass μ and used to build a relativistic scalar model for deuteron.

The results presented in this paper concern the S-wave bound states in the ladder approximation. They are aimed to (i) compare the LFD and Bethe-Salpeter descriptions and study their non relativistic limits, (ii) disentangle

the origin of the different relativistic effects, *(iii)* evaluate the contribution of higher Fock components and *(iv)* apply this study to a scalar model for deuteron.

2 Equation for Wick-Cutkosky model

We have considered the following lagrangian density:

$$\mathcal{L} = \frac{1}{2} \left(\partial_\nu \phi \partial^\nu \phi - m^2 \phi^2 \right) + \frac{1}{2} \left(\partial_\nu \chi \partial^\nu \chi - \mu^2 \chi^2 \right) - g \phi^2 \chi$$

where ϕ and χ are real fields. In the case $\mu = 0$ it corresponds to the Wick-Cutkosky model. The wave function Ψ , describing a bound state of two particles with momenta k_1 and k_2 , satisfies in the Light-Front the dynamical equation [7,5]

$$[4(q^2 + m^2) - M^2] \Psi(\vec{q}, \hat{n}) = -\frac{m^2}{2\pi^3} \int \frac{d^3 q'}{\varepsilon_{q'}} V(\vec{q}, \vec{q}', \hat{n}, M^2) \Psi(\vec{q}', \hat{n}) \quad (1)$$

Variable \vec{q} is the momentum of one of the particles in the reference system where $\vec{k}_1 + \vec{k}_2 = 0$, and tends in the non relativistic limit to the usual center of mass momentum. M represents the total mass of the composite system, $B = 2m - M$ denotes its binding energy and $\varepsilon_q = \sqrt{q^2 + m^2}$. In the case of S-waves the wavefunction is a scalar quantity depending only on scalars q and $\hat{n} \cdot \vec{q}$ [7,5].

The interaction kernel V calculated in the ladder approximation is given by

$$V(\vec{q}, \vec{q}', \hat{n}, M^2) = -\frac{4\pi\alpha}{Q^2 + \mu^2} \quad (2)$$

with

$$Q^2 = (\vec{q} - \vec{q}')^2 - (\hat{n} \cdot \vec{q})(\hat{n} \cdot \vec{q}') \frac{(\varepsilon_{q'} - \varepsilon_q)^2}{\varepsilon_{q'} \varepsilon_q} + \left(\varepsilon_q^2 + \varepsilon_{q'}^2 - \frac{M^2}{2} \right) \left| \frac{\hat{n} \cdot \vec{q}'}{\varepsilon_{q'}} - \frac{\hat{n} \cdot \vec{q}}{\varepsilon_q} \right|$$

The coupling parameter α is defined by $\alpha = g^2/16\pi m^2$. In the limit $\varepsilon_b \ll 2m$ some analytical solutions are known [15] and once removed the \hat{n} dependence in the kernel – formally setting $\hat{n} = 0$ – the LFD equation turns back to the Schrödinger equation in the momentum space for the Yukawa or Coulomb potential, α being the usual fine structure constant.

Equation (1) has been solved with the coordinate choice displayed in figure 1. We have chosen z axis along \hat{n} and with no loss of generality $\varphi = 0$. The φ'

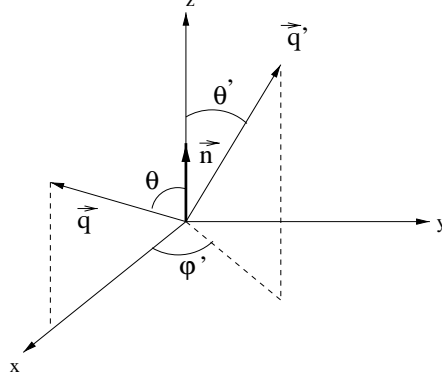


Fig. 1. Kinematical variables. The z axis is chosen along \hat{n} and \vec{q} can be restricted to the xOz plane without loss of generality

dependence of the kernel (2) can be performed analytically and (1) turns into the two dimensional integral equation

$$[4(q^2 + m^2) - M^2]\Psi(q, \theta) = \frac{4m^2\alpha}{\pi} \int \frac{q'^2}{\varepsilon_{q'}} dq' \sin \theta' d\theta' \frac{1}{\sqrt{a^2 - b^2}} \Psi(q', \theta') \quad (3)$$

with

$$\begin{aligned} a &= q^2 + q'^2 - qq' \left(2 \cos \theta \cos \theta' + \frac{(\varepsilon_{q'} - \varepsilon_q)^2}{\varepsilon_q \varepsilon_{q'}} \right) \\ &+ \left(q^2 + q'^2 + 2m^2 - \frac{M^2}{2} \right) \left| \frac{q' \cos \theta'}{\varepsilon_{q'}} - \frac{q \cos \theta}{\varepsilon_q} \right| + \mu^2 \\ b &= 2qq' \sin \theta \sin \theta' \end{aligned}$$

The kernel of (3) has an integrable singularity for $(q, \theta) = (q', \theta')$. The equation is solved by expanding the solution on a spline functions basis S_i , associated with coordinates q and θ : $\Psi(q, \theta) = \sum_{i,j} c_{ij} S_i(q) S_j(\theta)$. The r.h.s. two-dimensional integral is evaluated using Gauss quadrature method adapted to treat the singularity. The unknowns of the problem are the coefficients c_{ij} , which are solutions of a generalized eigenvalue problem $\lambda BC = A(M^2)C$ for M^2 values such that $\lambda(M^2) = 1$.

3 Results

The LFD binding energy for $\mu = 0$ versus the coupling constant is displayed in figure 2 (solid line). It is compared with the non relativistic values (dot-dashed

line) and a first order perturbative calculation B_{pert} (dashed line), valid also for Bethe-Salpeter (BS) equation [16], given by

$$B_{pert} = \frac{m\alpha^2}{4} \left(1 + \frac{4}{\pi} \alpha \log \alpha \right) \quad (4)$$

Corresponding numerical values – in $\hbar = c = m = 1$ units – are given in table 1 together with the quantity $R = \frac{\langle q^2 \rangle}{m^2}$ usually used to evaluate the relativistic character of a system. A first sight at this figure shows a significant departure

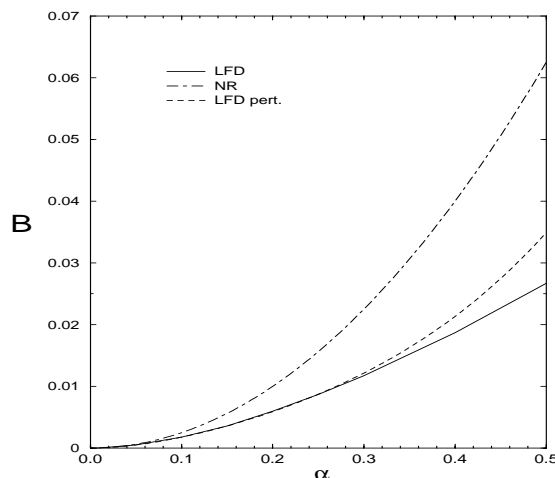


Fig. 2. Binding energy (solid) for $\mu = 0$ compared to non relativistic (dot-dashed) and perturbative (dashed) calculations

from the non relativistic results already for $\alpha = 0.1$. This discrepancy – which keeps increasing till B reaches the maximum value of $2m$ – is of 100% for $\alpha = 0.3$ whereas R remains very small. When evaluated using non relativistic solutions, R is equal to B (virial theorem), what gives $R \approx 2\%$ for $\alpha = 0.3$, in contrast with the 100% effect in the binding. The R values obtained using the LFD solutions are even smaller (see table 1). It is worth noticing the sizeable relativistic effects observed in a system for which both the binding energy and the average momentum are small.

A good agreement with the perturbative calculation is found up to values $\alpha \approx 0.3$ where the relative differences are 3%. The particular form of equation (4) ensures the existence of a non relativistic limit, the same for LFD and BS approaches, for the weakly bound states. We will see later on, that this situation is particular to the case $\mu = 0$.

The bound-state wavefunctions presented below are normalized according to

$$\frac{m}{(2\pi)^3} \int |\Psi(q, \theta)|^2 \frac{d^3q}{\varepsilon_q} = 1 \quad (5)$$

Table 1

Binding energies for $\mu = 0$ and $\mu = 0.15$ as function of the coupling constant α												
α	0.3	0.4	0.5	1.0	2.0	3.0	4.0	5.0	6.0	6.98	7.26	
$10^2 B_{\mu=0}$	1.17	1.87	2.67	7.68	21.0	38.0	58.5	84.0	118	200	-	
$10^2 \frac{\leq q^2 \geq}{m^2}$	1.1	1.8	2.5	6.7	17	28	40	55	64	80	-	
$10^2 B_{\mu=0.15}$	-	0.190	0.570	4.36	16.5	32.7	-	75.6	107	157	200	

with $\varepsilon_q = m$ for the non relativistic case. The LFD wave function $\Psi(q, \theta = 0)$ obtained for $\alpha = 0.5$ is compared in figure 3a (solid line) with the corresponding non relativistic solution (dot-dashed line), that is Coulomb wave function. The sizeable difference between both functions is mainly due the differences in their binding energies: $B_{LFD} = 0.0267$ whereas $B_{NR} = 0.0625$ for the same coupling constant. In order to compare wave functions with the same energy, the value of the coupling constant for the non relativistic solution is adjusted to $\alpha_{NR} = 0.327$. The wave function obtained (long-dashed curve) is then much closer to the relativistic one.

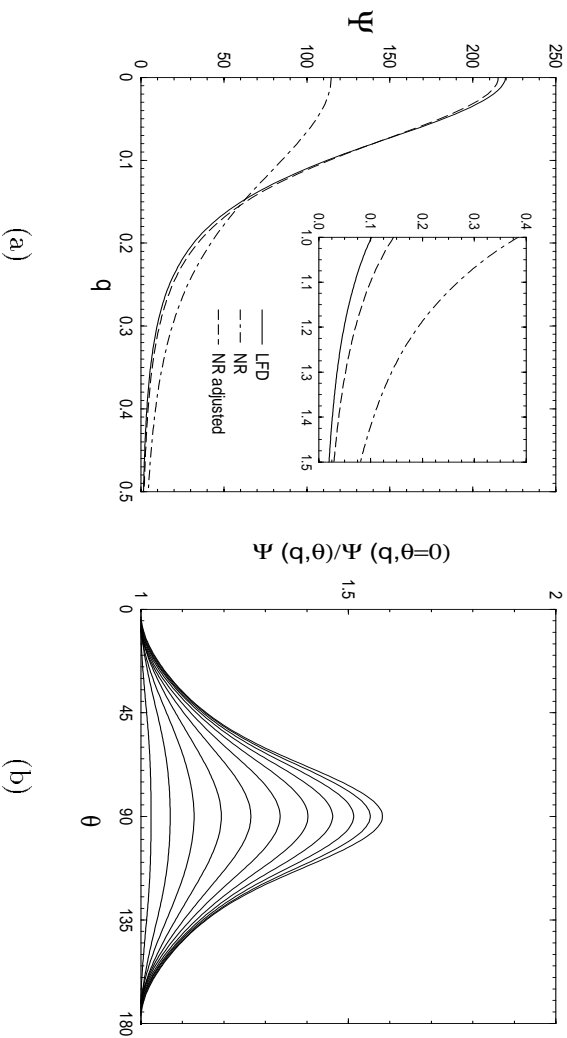


Fig. 3. (a) S-wave LFD solution for $\theta = 0$ (solid) compared with Coulomb wave function with the same coupling constant (dot-dashed) and the same energy (dashed). Figure (b) shows the angular dependence of the wave function for different values of q . Curves from bottom to top correspond to increasing momenta from $q = 0$ to $q = 1.5$.

Furthermore, in the region of high momentum transfer, the relativistic function is smaller than the Coulomb one, as expected from the natural cut-off of high momentum components introduced by relativity. However, these differences can be accounted with the θ dependence of the LFD solutions, which exists even for S-waves. This angular dependence, normalized by the value of $\Psi(q, \theta = 0)$, is shown in figure 3b for different values of momentum $0 \leq q \leq 1.5$.

As one can see, the influence of the momentum orientation compared to the light-front plane is far from being negligible. This effect increases with q and, for a fixed value of the momentum, is maximum when $\hat{q} \cdot \hat{n} = 0$. For this kinematical configuration, i.e. relative momentum in the Light-Front plane, the relativistic wave function $\Psi(q, \theta = 90^\circ)$ at high momentum is even found to be bigger than non relativistic one. To get rid of this dependence, we compared $|\Psi(q, \theta)|^2$ integrated over the θ degree of freedom, both for relativistic and non relativistic solutions. The resulting functions, displayed in figure 4, measure the effective relativistic effects in the wavefunctions. At $q = 0$ they remain at the level of 5%, once the energy is readjusted. In the high momentum region the relativistic solution is – as expected – smaller than the non relativistic one, but their differences reach a factor three at $q = 2$, and this for a moderate value of the coupling constant $\alpha = 0.5$.

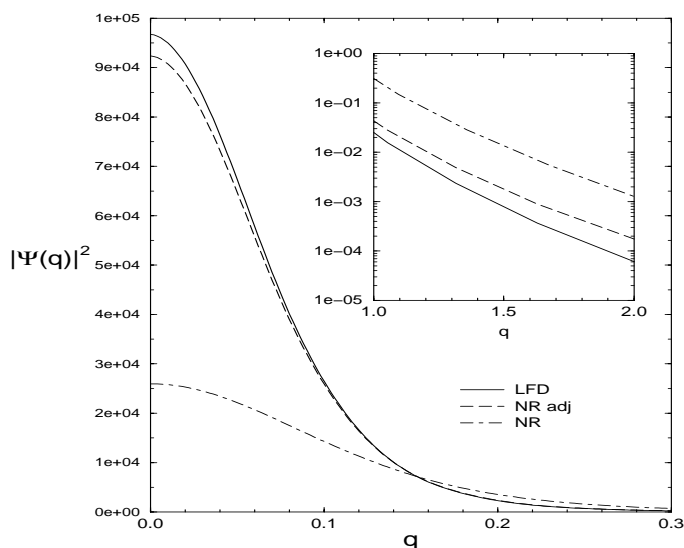


Fig. 4. Squared modulus of the wave function integrated over θ . The LFD solution (solid line) and the reajusted non relativistic one (dot-dashed line) have same binding energy. The small top right graph is a zoom of the high momentum region.

In the case $\mu \neq 0$ there exists a critical α_0 below which there is no bound solution. Figure 5 represents the binding energy B as a function of the coupling constant α for different values of μ . They are compared with those provided by BS equation in the same ladder approximation, whose kernel incorporates higher order intermediate states. We have solved this equation using the method described in [17]. A first remark in comparing both approaches is that their results are seen to be close to each other. This fact is far from being obvious – specially for large values of coupling constant – due to the differences in their ladder kernel. A quantitative estimation of their spread can be given by looking into an horizontal cut of figure 5, i.e. calculating the relative difference in the coupling constant $(\alpha_{LFD} - \alpha_{BS})/\alpha_{LFD}$ for a fixed value of

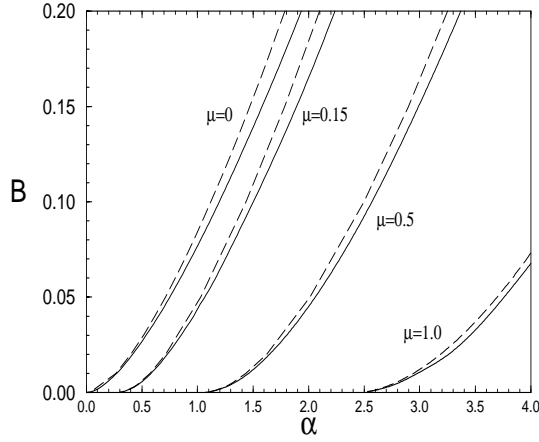


Fig. 5. Binding energy as a function of α for different values of μ in LFD (solid) and BS (dashed) approaches

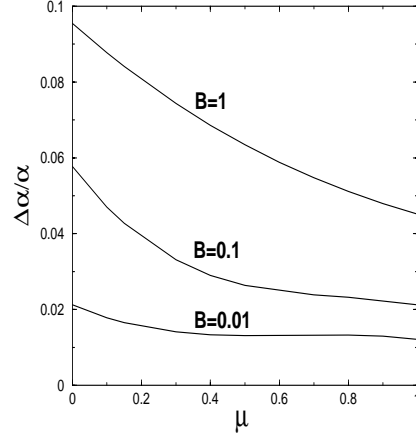


Fig. 6. Differences in the coupling constant as a function of μ for fixed values B .

the binding energy. The results, displayed in figure 6 for $B = 1.0, 0.1, 0.01$, show that relative differences (i) are decreasing functions of μ for all values of B (ii) increase with B but are limited to 10% for the strong binding case $B = m$ which involves values of $\alpha \geq 5$. This indicates the relatively weak importance of including higher Fock components in the ladder kernel even for strong couplings, as already discussed in [13].

It is interesting to study the weak binding limit of both relativistic approaches and compare them with the non relativistic calculations in the case $\mu \neq 0$. The results are given in figure 7a for $\mu = 1$. They show on one hand that LFD and BS (solid lines) converge towards very close, though slightly different, values of the coupling constant ($\frac{\Delta\alpha}{\alpha} \approx 0.01$). On the other hand one can see, contrary to the $\mu = 0$ case in figure 2, a dramatic departure of both relativistic approaches from a non relativistic theory (dot-dashed line), even for negligibles values of binding energy. The differences increase with μ as shown in figure 7b in which LFD and BS results are not distinguished. The origin of this departure lies in the fact that the integral term in equation (1) is dominated by the region $q' \sim \mu$, even for very small values of B , and for the case $\mu \sim m$ the $\frac{q'}{m}$ terms – which make the difference between the non relativistic and relativistic kernels – are not longer negligible. We conclude from that to the non adequacy of a non relativistic treatment in describing systems interacting via massive fields, what is the case of all the strong interaction physics when not described via gluon exchange.

Some approximations of equation (1) have been studied in order to disentangle the different contributions to the relativistic energies $B(\alpha)$ (see figure 8). Equation (1) is formally written $K\Psi = \frac{1}{\varepsilon_q} V\Psi$. We first consider the case of a non relativistic kernel V – i.e. a Yukawa potential – and $\varepsilon_q = m$, with

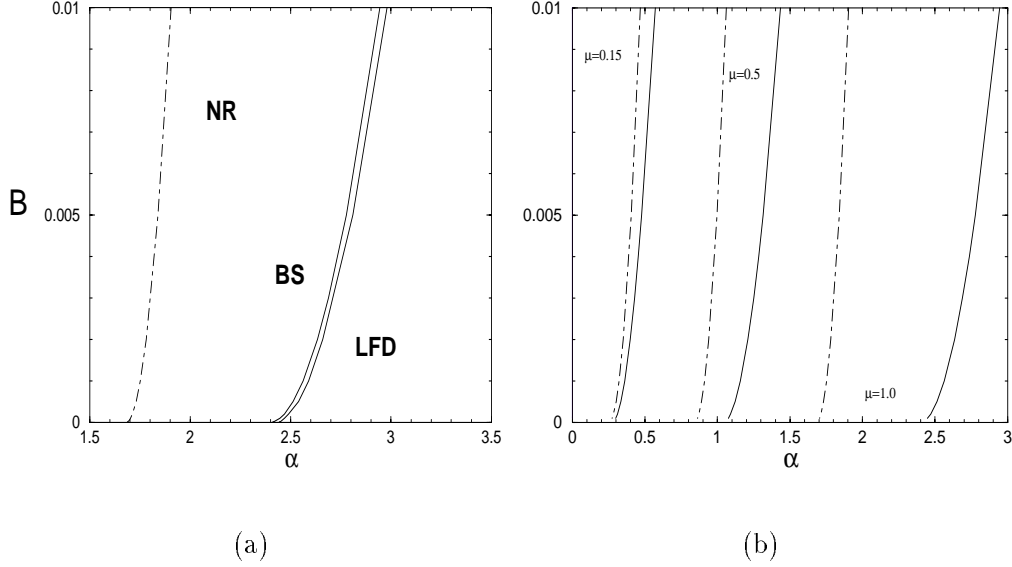


Fig. 7. Zero binding energy limit of LFD and BS equations (solid) compared with the non relativistic solutions (dot-dashed) for $\mu = 1$ (a) and for different values of μ (b).

in curve a the non relativistic kinematics $K = 4q^2 + 2mB$ and in curve a' the relativistic one $K = 4(q^2 + m^2) - M^2$. Curves b and b' are obtained in the same manner, but putting $\varepsilon_q = \sqrt{q^2 + m^2}$. The last one corresponds to the LFD equation. The results in figure 8 show that the kinematical term K has a very small influence on $B(\alpha)$, whereas the contributions of ε_q and V to the total binding are both essential. We conclude from this study that the kinematical corrections alone, as they are performed e.g. in minimal relativity calculations, are not representative of relativistic effects. Even by including them in the kernel through ε_q the results obtained are wrong by a factor 2.

In case of an energy dependent kernels the normalization condition (5) is only approximate. This energy dependence denotes coupling to higher Fock components and the correct normalization condition for the model considered reads $N^{(2)} + N^{(3)} = 1$ where $N^{(3)}$ is the norm contribution from the three-body Fock component. Using (5) only the two-body part is included. One can show that the correction $N^{(3)}$ to the two-body normalization condition is given by:

$$N^{(3)} = -\frac{4m^2}{(2\pi)^6} \int \frac{d^3q}{\varepsilon_q} \frac{d^3q'}{\varepsilon_{q'}} \Psi^*(q', \vec{q}' \cdot \hat{n}) \frac{\partial V}{\partial M^2}(\vec{q}, \vec{q}', \hat{n}, M^2) \Psi(q, \vec{q} \cdot \hat{n}) \quad (6)$$

This expression can be analytically integrated over two angles φ and φ' and we are left with a four dimensional integration. The three-body correction to the norm, i.e. the ratio $\frac{N^{(3)}}{N^{(2)} + N^{(3)}}$, as a function of the coupling constant is

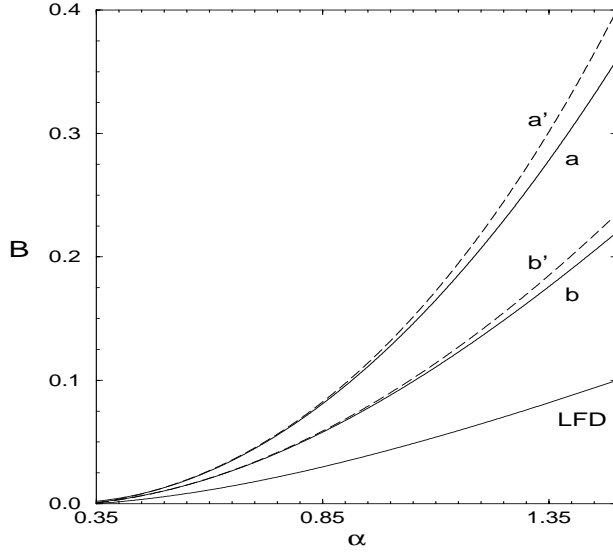


Fig. 8. Relativistic contributions of different terms in equation (1) (see text)

shown in figure 9 for the case $\mu = 0.15$. We remark that this correction is not zero at the critical value $\alpha = 0.35$ corresponding to the $B = 0$ threshold. Its behaviour in the region of large coupling tends asymptotically towards a value non exceeding 30%. This is in contrast with the evolution of the parameter R introduced in the same figure to estimate the norm correction for a system with a given value of R . For deuteron, e.g., one has $R \approx 1\%$ and the expected normalization corrections are of the order of 4%.

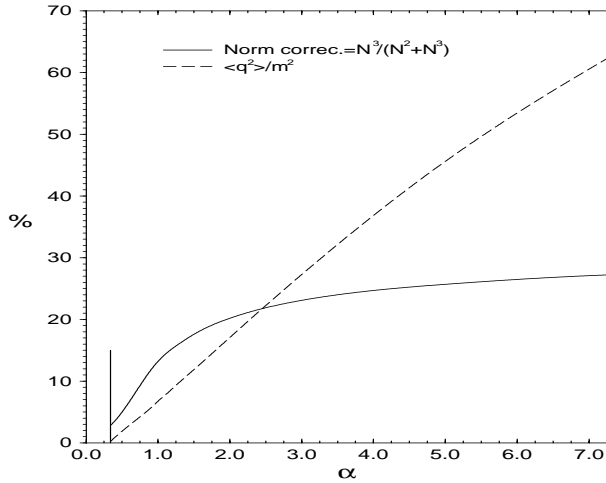


Fig. 9. Normalization correction due to 3-body Fock components and relativistic parameter $R = \frac{\langle q^2 \rangle}{m^2}$ as functions of α for the case $\mu = 0.15$.

4 A scalar model for Deuteron

A simple relativistic model for deuteron in the LFD is obtained by adding to the interaction kernel (2) a repulsive part exactly analogous except for the sign of the coupling constant. Even if this procedure is no longer based on field theory – a scalar exchange cannot produce a repulsive interaction – the potential obtained constitutes a LFD relativistic version of the Malfliet and Tjon NN potential [18] on the form:

$$V(\vec{q}, \vec{q}', \hat{n}, M^2) = \frac{V_R}{Q^2 + \mu_R^2} - \frac{V_A}{Q^2 + \mu_A^2} \quad (7)$$

The non relativistic model corresponds to $Q^2 = (\vec{q} - \vec{q}')^2$ and for the 3S_1 state the parameter set $V_R=7.29$, $V_A=3.18$, $\mu_A=0.314$ GeV, $\mu_R=2\mu_A$ inserted in Schrödinger equation ensures a deuteron binding energy $B = 2.23$ MeV.

By solving the LFD equation (1) with potential (7) we can estimate the modification in the deuteron description due to a fully relativistic treatment. The first result concerns its binding energy which becomes $B = 0.96$ MeV. The inclusion of relativity produces thus a dramatic repulsive effect, already drawn in [19]. We emphasize that, as mentioned before in the case of Wick-Cutkosky model, the use of relativistic kinematics alone induces a very small change in the binding energy. The sizeable energy decrease is almost entirely due to the r.h.s. part of (1). To obtain a proper deuteron description in a relativistic frame it is necessary to readjust the parameters of the non relativistic model. A binding energy of 2.23 MeV is recovered with a repulsive coupling constant $\Lambda_R = 6.60$ MeV – all other parameters being unchanged – what represents an decrease of 10% with respect to its original value. Another possibility is to increase the attractive coupling constant up to $V_A = 3.37$. The relativistic effects in deuteron wave function depend sensibly on the way the energy is readjusted as well as on the relative angle θ between \hat{n} and the momentum \vec{q} . For instance when modifying V_A and for the value $\theta = 0$, the zero of the relativistic wave function is shifted by ≈ 0.1 GeV/c towards smaller values of q and the differences in the momentum region of $q = 1.5$ GeV/c are 50% in amplitude.

5 Conclusion

We have obtained the solutions for a scalar model in the Light Front Dynamics framework and in the ladder approximation. The results presented here concern the S-wave bound states.

We have found that the inclusion of relativity has a dramatic repulsive effect on binding energies even for systems with very small $\frac{\langle q \rangle}{m}$ values. The effect is specially relevant when using a scalar model for deuteron: its binding energy is shifted from 2.23 MeV down to 0.96 MeV. This can be corrected by decreasing of 10% the repulsive coupling constant, what indicates the difficulty in determining beyond this accuracy the value of strong coupling constants within a non relativistic framework.

Light-Front wave functions strongly differ from their non relativistic counterparts if they are calculated using the same values of the coupling constant. Once the interaction parameters are readjusted to get the same binding energy both solutions become closer but their differences are still sizeable.

The relativistic effects are shown to be induced mainly by the relativistic terms of the kernel. The relativistic kinematics has only a small influence on the binding energy; furthermore, its effect is attractive whereas the total relativistic one is strongly repulsive.

The normalization corrections due to the three-body Fock components increase rapidly for small values of the coupling constant and saturate at $\approx 25\%$ in the ultra relativistic region. They have been estimated to 4% in the deuteron.

The LFD results are very close to those provided by Bethe-Salpeter equation for a wide range of coupling constant despite the different physical input in their ladder kernel. However in the case of systems interacting via a massive exchanged field, they both strongly differ from the non relativistic solutions even in the zero binding limit. This leads to the conclusion that such systems cannot be properly described by using a non relativistic dynamics.

The case of higher angular momentum states for scalar particles requires more formal developments and is presented in a forthcoming publication [20].

Acknowledgement

We are grateful to V.A. Karmanov for enlightening discussions during this work and for a careful reading of the manuscript. We thank L. Theussl for providing some results from [14] prior to its publication

References

- [1] P.A.M. Dirac, Rev. Mod. Phys. 21 (1949) 392

- [2] B.D. Keister, W.N. Polyzou, Adv. in Nucl. Phys. Vol. 20 (1991) 225
- [3] F. Coester, Prog. Part. Nucl. Phys. **29** 1 (1992)
- [4] M. Burkardt, Adv. in Nucl. Phys. Vol. **23** (1996) 1-74
- [5] J. Carbonell, B. Desplanques, J.F. Mathiot, V.A. Karmanov, Phys. Rep. 300 (1998) 218
- [6] S. J. Brodsky, H-C. Pauli, S.S. Pinsky, Phys. Rep. 301 (1998) 299
- [7] V.A. Karmanov, Sov. Phys. JETP 44 (1976) 210
- [8] J. Carbonell and V.A. Karmanov, Eur. Phys. J. A6 (1999) 9
- [9] G.C. Wick, Phys. Rev. 96 (1954) 1124; R.E. Cutkosky Phys. Rev. 96 (1954) 1135
- [10] T. Nieuwenhuis and J.A. Tjon, Phys. Rev. Lett. 77 (1996) 814
- [11] J. Darewich, Can. J. of Phys. **76** (1998) 523; M. Barham and J. Darewich, J. Phys. A **31** (1998) 3481-3491
- [12] T. Frederico, J.H.O. Sales, B.V. Carlson, P.U. Sauer, Few-Body Systems Suppl. 10 (1998) 123; Preprint nucl-th 9909029
- [13] N. Schoonderwoerd, B.L.G. Bakker, V.A. Karmanov, Phys. Rev. C 58 (1998) 3093; N. Schoonderwoerd, PhD. Thesis, Vrije Universiteit Amsterdam (1998)
- [14] L. Theussl and B. Desplanques, nucl-th/9908007
- [15] V.A. Karmanov, Nucl. Phys. B166 (1980) 378
- [16] G. Feldman, T. Fulton, J. Townsend, Phys. Rev. **D7** 1814 (1973)
- [17] T. Nieuwenhuis and J.A. Tjon, Few-Body Systems 21 (1996) 167
- [18] R.A. Malfliet, J.A. Tjon, Nucl. Phys. A 127 (1969) 161
- [19] P. Danielewicz and J.M. Namyslowski, Phys. Lett 81B (1979) 110
- [20] M. Mangin-Brinet, J. Carbonell and V.A. Karmanov, submitted to publication